CHARACTERIZATION OF ALLOY 82/182 DISSIMILAR WELD METAL USED BETWEEN ASTM A-508 LOW ALLOY STEEL AND 316L STAINLESS STEEL

Luciana Iglésias Lourenço Lima, lill@cdtn
Alexandre Queiroz Bracarense, bracarense@ufmg.br
Angel Raphael Arce Chilque, anarcec@yahoo.com
University Federal of Minas Gerais - UFMG. Av Antônio Carlos, 6627 Campus Pampulha BH-MG

Mônica Maria de Abreu Mendonça Schvartzman, monicas@cdtn.br
Marco Antônio Dutra Quinan, quinanm@cdt.br
Nuclear Technology Development Centre- CDTN. Av Antônio Carlos, 6627 Campus Pampulha BH-MG

Guilherme Marconi Silva, guilherme.marconi@terra.com.br
Federal Center of Technological Education, CEFET-MG. Av Amazonas, 7675 Nova Gameleira BH-MG

Abstract..*Welds used to joint different metals are known as dissimilar welds and are used in several areas of industries. In nuclear power plant, this weld is used to joint stainless steel nipples to carbon steel components on the reactor pressured vessels. In components of Brazilian nuclear power plant Angra 1 nickel-based alloys (alloy 182 and alloy 82) are used in dissimilar welds in nozzles of the reactor pressure vessel and the pressurizer. Despite its high corrosion resistance and good mechanical properties, it presented, after long operation period, susceptibility to stress corrosion crack (SCC) in a primary circuit of a nuclear pressurized reactor (PWR). SCC is a thermally activated process that occurs if the following three conditions occurs simultaneously: susceptible material, corrosive environment and the presence of tensile stress. The material microstructure plays an important role in this phenomenon. Susceptible microstructures can include interdendritic boundaries and grain boundaries containing segregated or precipitated impurities and solidification microstructures caused by welding can futher complicate the stress corrosion crack behavior. In this study, dissimilar metal welds composed of ASTM A-508 low carbon steel and AISI 316L austenitic stainless steel, as base metal, and 182/82 nickel alloys, as a filler metal, were prepared using gas tugsten arc welding (GTAW) and shielded metal arc welding (SMAW) techniques. Metallographic properties of the weld were obtained by means of microhardness test, optical and scanning microscopy (SEM) combined with energy-dispersive x-ray spectrometer (EDS). The corrosion behavior of the weld metal and base metal were investigated by potentiodynamic anodic polarization technique, that is used to determine the active/passive characteristics of a given metal-solution system. The results indicated that alloy 82 has a weak passivity that could could be attributed to the chromium depletion in the regions adjacent to the grain boundary. The results also indicated that the base metal ASTM A508 has the weakness passivity what is compatible behavior of the alloy steel.*

Keywords*: dissimilar metal weld, nickel-based alloy 182/82, microstructural characterization*

1. INTRODUCTION

The welds used to join different metals are known as dissimilar metal welds (DMW) and are used in several areas of industries. In the nuclear power plant, this weld is used to connect stainless steel nipples to ferritic steel components on the reactor pressured vessels. The type and the characteristics of the DMW depend on a range of factors; some of them are the specific reactor design, the welding procedure and the weld material (Miteva and Taylor, 2006).

Nickel-base alloys weld metals, such alloys 82 and 182, are used as a consumable in DMW involving ferritic and stainless steel base materials due their thermal expansion coefficients that rank between those of the ferritic and austenitic base materials, the reduced carbon diffusion because of the reduced carbon activity gradient between it and the ferritic steel, the corrosion resistance and the combination of good mechanical properties and fracture toughness (Sireesha et al., 2000). Those alloys were originally selected to be used in components of Brazilian nuclear power plants Angra 1 and Angra 2, as dissimilar welds in nozzles of reactor pressure vessel and the pressurizer.

Despite its high corrosion resistance, it presented, after long operation period, susceptibility to stress corrosion crack (SCC) in a primary circuit of a nuclear pressurized water reactor (Pathania, et.al, 2002, Banford and Hall, 2004, Scott, 2004). SCC is a form of environmentally assisted cracking (EAC). EAC refers to a phenomenon by which a normally ductile metal loses its toughness when it is subjected to mechanical stresses in presence of a specific corroding environment. For EAC and consequently SCC to occur, three affecting factors must be present simultaneously. These are: mechanical tensile stresses, susceptible metal microstructure and a specific aggressive environment. If any of these three factors is removed, EAC and SCC will not occur (Rebak, 2005).

The microstructure of the material and its electrochemical behavior plays an important role in stress corrosion cracking. Susceptible microstructures can include hot cracks as well as interdendritic boundaries and grain boundaries containing segregated or precipitated impurities. Solidification microstructures caused by welding can further complicate SCC behavior (EPRI, 2005, Gomes- Briceño, 2005). Some stress corrosion mechanisms, involving localized dissolution of the alloy when the oxide layer cracks, are directly related to the electrochemical properties of the alloy. Stress corrosion occurs in potential ranges where the passive layers are not very stable, in particular around the Ni/NiO equilibrium and when the passivated surface is damaged by stress (Le-Canut, 2004).

This work includes the characterization of the alloys 82/182 used as dissimilar metal weld between low alloy carbon steel ASTM A-508 and 316L stainless steel. Metallographic properties of the specimens were obtained by means of microhardness testing, and optical and scanning electron microscopy (SEM) combined with energy-dispersive spectrometer (EDS). The corrosion behavior of the weld metal and base metal were investigated by potentiodynamic anodic polarization technique, that is used to determine the active/passive characteristics of a given metal-solution system.

2. MATERIALS

Plates of alloys ASTM A-508 class 3 and AISI 316L were used to construct the dissimilar metal weld. The chemical compositions of the base and filler metals are given in Tab. 1. Table 2 shows the mechanical properties of the materials. The plates are manually welded, reproducing the welding procedures used for the nozzle to pipe welding in the Brazilian power plant Angra 1. The J groove weld was prepared by joining two 130 x 300 mm pieces of 36 mm (ASTM A-508 class 3) and 31 mm (AISI 316L) thick plate (Fig. 1). Before the welding, 5 buttering passes were applied on the ASTM A-508 plate side by manual GTAW with alloy 82. The resulting buttering thickness was about 5 to 8 mm. After buttering the piece was machined and post welding heat treated at 600ºC during 2 hours. The pieces were pre heated at 150ºC before the welding and the maximum inter-pass temperature during the welding was 200ºC. The final weld had 3 root passes made with 82 alloy wire with GTAW and 37 passes made with 182 electrode with SMAW. The conditions used to produce each weld pass are listed in Tab. 3. The finished weld blocks was not heat treated. Figure 2 shows the buttering and the finished weld plate. After welding, the welded joint was cut in pieces for microstructural observation and microhardness test according to ASTM E6 and ASTM E384.

Table 1 – Chemical composition of the base and weld metals

	C	**Mn**	**Si**	**P**	**S**	**Cr**	**Ni**	**Nb**	**Ti**	**Cu**	**Mo**	**Al**	**Fe**
316L	0,023	1,458	0,475	0,021	0,003	16,732	9,834	0,0199	0,029	0,142	2,097	0,011	68,93
ASTM A 508	0,213	1,336	0,227	0,005	0,003	0,089	0,682	0,002	0,001	0,0559	0,505	0,011	96,83
182*	0,047	5,810	0,572	0,015	0,006	14,930	71,820	1,890	0,183	0,019	-	-	4,59
82**	0,04	2,81	0,09	0,003	0,001	19,6	73,10	2,44	0,35	0,01	-	-	1,29

* Manufacturer´s Qality Certificated – Novametal do Brasil Ltda. ** Manufacturer´s Qality Certificated – Kestra Universal Soldas.

Table 2 –Materials Mechanical Properties.

	Yield Strength $LE_{0,2\%}$ (MPa)	**Ultimate Tensile Stress (MPa)**	**Enlogation (%)**
ASTM A 508	345	550 - 725	18
316L	170	485	40
82	385	530	30
182	425	576	18

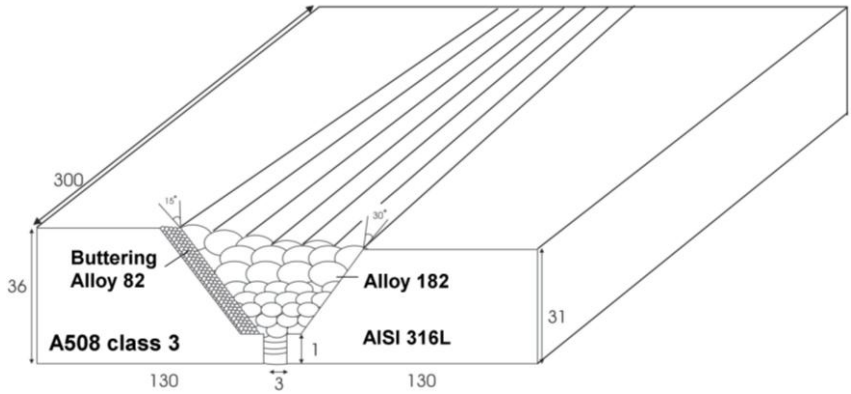

Figure 1 - A schematic of the weld design.

Table 3 – Welding process and conditions for the various welding passes.

Welding Passes	Process	Filler Metal	Electrode size (mm)	Current (A)	Voltage (V)	Travel speed (mm/s)
Buttering	GTAW	82	2,5	90 - 130	17,5 - 18	1,8 – 3,0
1 - 3	GTAW	82	2,5	126 - 168	20 - 22	1 – 1,2
4 - 37	SMAW	182	4	119 - 135	22 - 26	1 – 3,5

(a) (b)

Figure 2 – (a) the buttering layer applied on the ASTM A-508 base metal and (b) to view of the weld finished plate.

3. EXPERIMENTAL PROCEDURE

For the metallographic examination samples were cut and prepared grinding with waterproof SiC papers with a final grit size of 1200 and finally polished until 1 μm diamond paste and a chemical etching was applied. The chemical etchants and the etching conditions used are listed in Tab.4. The samples were investigated by optical and scanning electron microscopes in the plane of the picture and chemical composition mapping of the samples were done by EDS.

Table 4 – Chemical etching conditions.

Sample	Etching Conditions
ASTM A508	Nital 2% - 20 seconds (Immersion)
AISI 316	Fluoridric Acid 10% -1A, 2V, 60 seconds (Electrolytic Etching)
Alloy 182/82	Oxalic Acid 10% - 1A, 2V, 30 seconds (Electrolytic Etching)

Vickers microhardness profiles across the weld metal base metal interface were obtained at a constant load of 100g and loading time of 15 seconds. In Figure 3 the lines indicate the places where microhardness was performed.

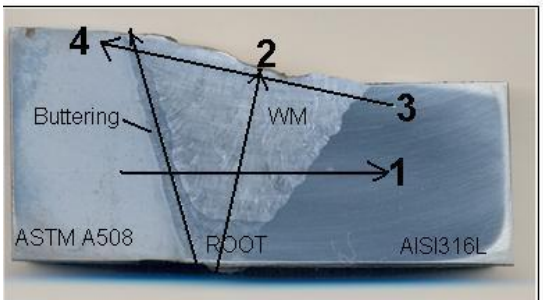

Figure 3 - Indication of the microhardness lines measurements.

Samples corrosion behavior was investigated by potentiodynamic anodic polarization using an Autolab PGSTAT 20 potentiostat with GPES 4.4 software. For comparison, samples were tested under identical conditions. They were prepared by epoxy hot resin and the surfaces, to be exposed to the electrolyte, were sequentially grinded with silicon carbide paper up to 600 mesh. Measurements were conducted in accordance with ASTM G5 (1994) standard in a conventional three electrode cell. The electrochemical cell consisted of the working electrode, an Ag/AgCl (1.0 mol.L^{-1}) reference electrode and a platinum counter electrode. Thus, all potentials cited in this study will be in reference to Ag/AgCl. The experimental temperature was controlled at 30±1ºC. The scans were carried out with a rate of 0.167 mV/s in the range from –200 mV to 2.000 mV with respect to the open circuit potential (OCP) in a de-aerated 0.5M H_2SO_4 solution. The tests were carried out in triplicate for each condition and comparing the results of all experiments.

4. RESULTS AND DISCUSSION

4.1. Metallographic characterization

The microstructure of the base metals is show in Fig.4. As can be observed the ASTM A508 steel is composed of a typical tempered bainite structure and the AISI 316L steel of a well-developed polygonal austenitic grains with a small amount of delta ferrite.

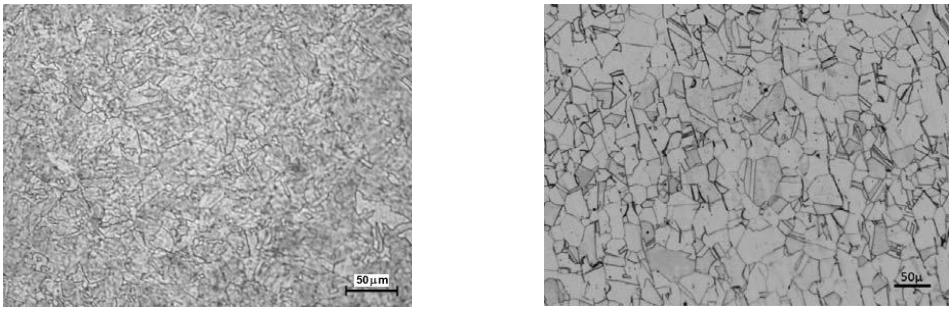

(a) (b)

Figure 4 – (a) microstructure of the ASTM A508 carbon steel and (b) microstructure of the AISI 316L stainless steel

Figure 5 (a) shows the interface between the ASTM A508 ferritic steel (black) and the Buttering (alloy 82), (b) the buttering region, (c) the microstructure of the root area, (d) the weld region and (e) the fusion boundary between alloy 182 and AISI 316L. As can be observed the microstructures of alloys 82 and 182 weld metals are fully austenitic. The dendritic microstructure is clear in the buttering area and in the weld region. The grain structure is columnar and forms in the heat flow direction, consistent with the studies conducted by Peng et. al (2007). The dendrites shapes depend on theirs position on the weld zone. They are more closely spaced at the bottom part compared with the upper part of the weld.

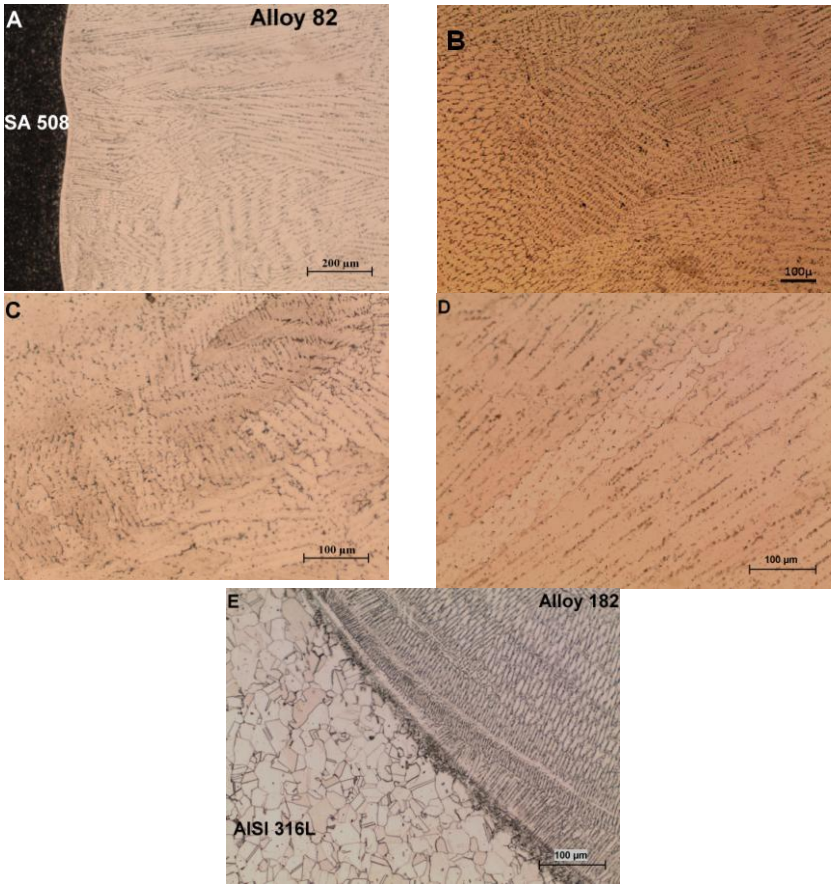

Figure 5 - Microstructure of dissimilar weld regions: a) Interface ASTM A508 (black)/A82(buttering); b) buttering (middle); c) root area – alloy 82; d) weld (alloy 182) and e) fusion boundary between alloy 182 and AISI 316L.

In the area around the dendrites and in the dendrites grain boundaries were observed some inclusions and precipitates. In order to investigation the composition of these inclusions and precipitates, energy dispersive X – ray spectrometer analysis (EDS) mapping were performed. Figure 6 shows photos where the analysis was performed and the distribution of alloying elements, silicon (Si), nickel (Ni), chromium (Cr), iron (Fe), niobium (Nb) and carbon (C) was investigated. In the figures a light colors represents a high element concentration. This mapping showed a concentration of niobium, chromium and carbon in the region of precipitates also suggesting the presence of niobium and chromium carbides. The precipitation occurs due the heat and cooling effects during the welding. With no or insufficient amounts of carbon stabilizing elements such as Nb and Ti, Cr carbides will precipitate. In contrast when sufficient amounts of Nb and Ti are present, the carbon in the matrix is consumed through the prevailing precipitation and growth of Nb and Ti carbides at high temperature (Kaneda, 2007).

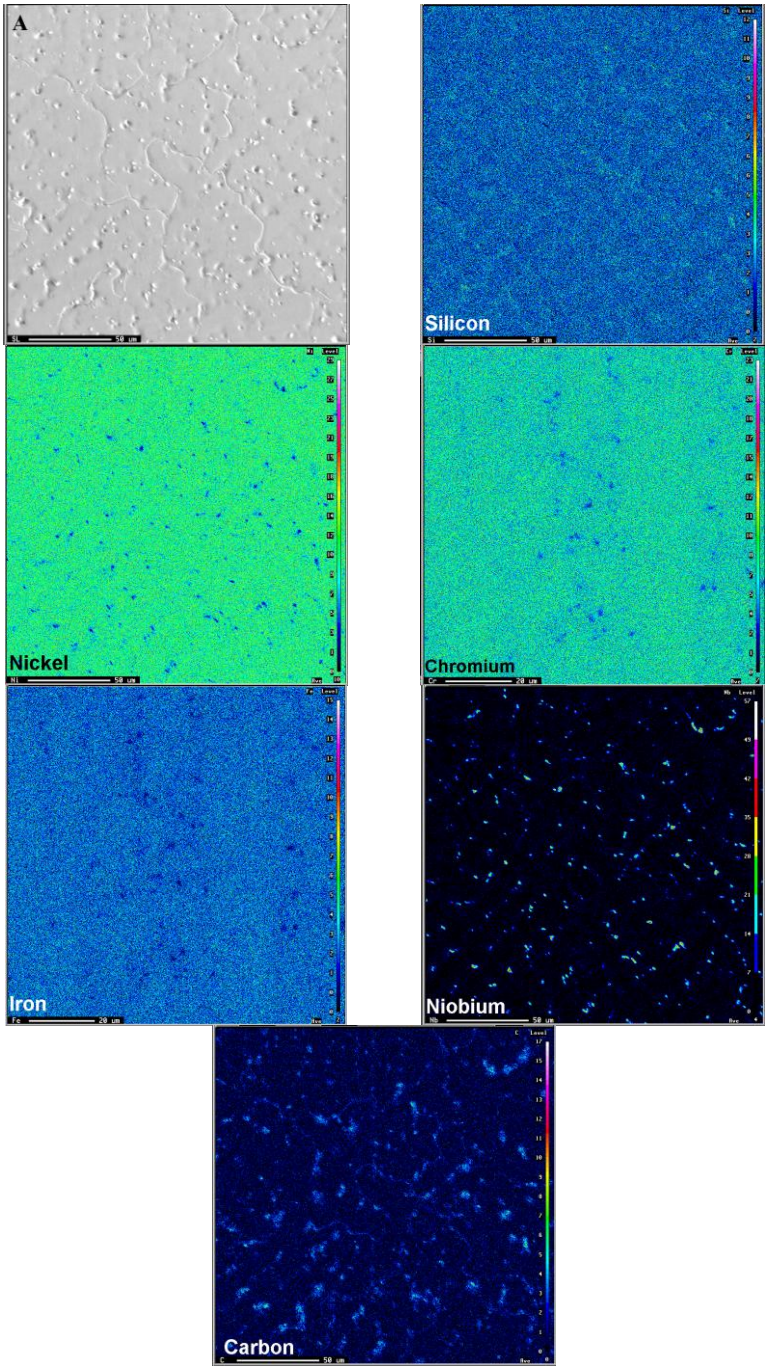

Figure 6 – Distribution of the elements Si, Ni, Cr, Fe, Nb and C in the weld.

In Fig. 7, the profile lines 1 and 3 show the distribution of the microhardness along the entire dissimilar welded joint. In particular the results showed that the microhardness Vickers (HV) in the heat affected zone (HAZ) of the ferritic steel is of the same order of the others parts of the welded joint. This means that the post welding heat treatment applied after buttering was appropriated to eliminate the quenched structure present in this region. These profiles together with the 2 and 4 profiles of weld metal and buttering region respectively, showed microhardness values changing from 180 to 270 HV. The continuous and relative smooth variation of the microhardness in the welded joint is similar to the tensile strength showed in Tab. 3. The results obtained for the dissimilar welded joint with the welding procedure designed show that it is possible to meet a good compromise between microstructures, mechanical properties and appropriate weldability of different regions with capacity to guarantee the integrity of the welded joint. It is still necessary to do a specific microstructural and microchemical study of the substructures of the different regions to explain some differences in the fusion line, root and weld pool zone caused by the multipass technique used.

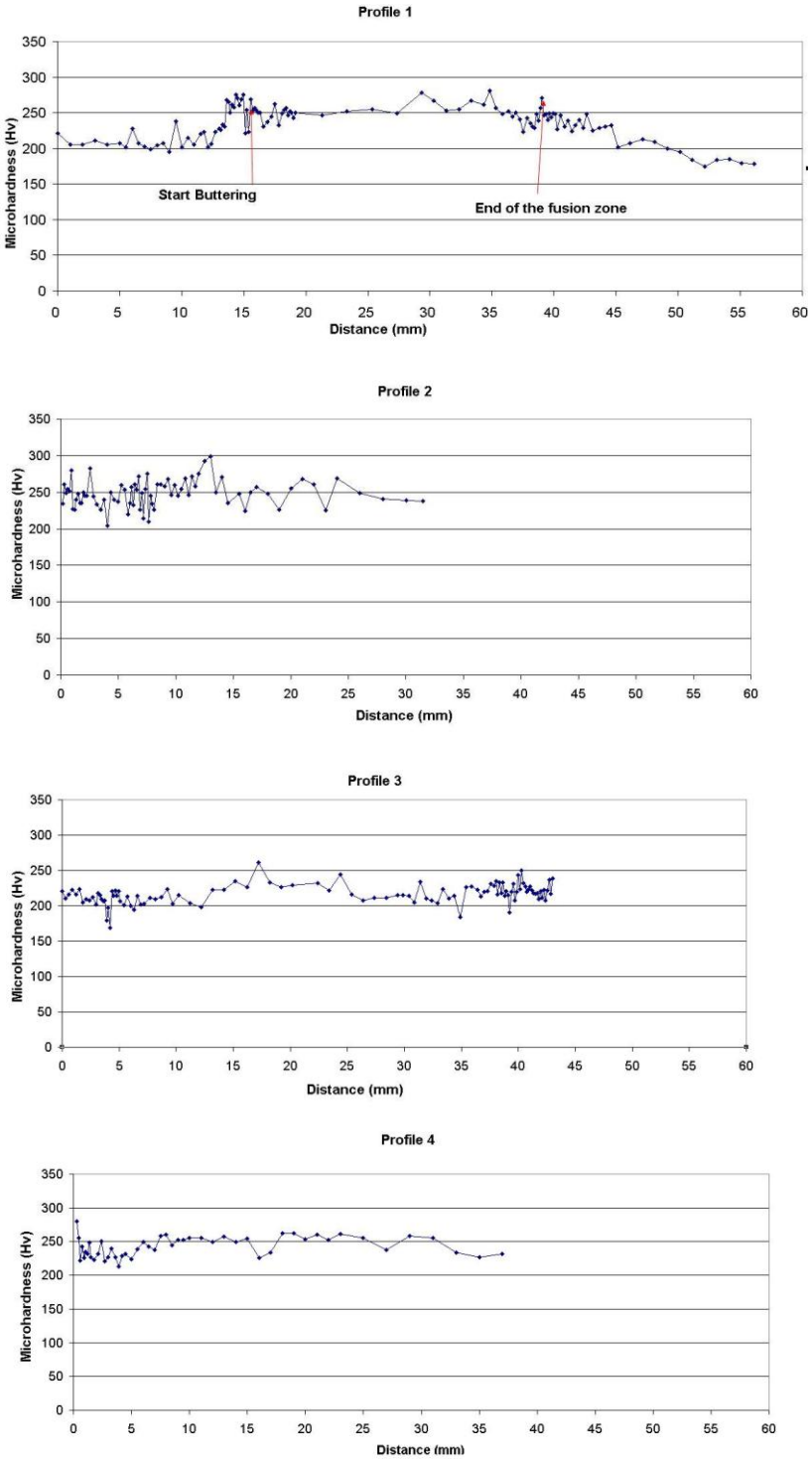

Figure 7 – Microhardness Vickers distribution in line 1 (a), line 2 (b), line 3 (c) and line 4 (d) showed in Figure 3.

4.2. Electrochemical characterization

Figure 8 shows the anodic polarization curves for the samples studied and the corrosion parameters are listed in Tab.5. The polarization curves show all similar behavior. Each curve has an "active-to-passive transition" and at more anodic potentials a transpassive region. It is clear that the current density in the passivation region showed different values. This indicated different passivation degrees. For the ASTM A508 base metal the current density was of the order of 10^{-4} A/cm². For the buttering, alloy 82, it was of 10^{-5} A/cm² and for the AISI 316L base metal and the weld metal alloy 182, of 10^{-6} A/cm². These results indicated the weak passivity of the ASTM A508 base metal and of the

buttering region (alloy 82). For the ASTM A508 this behavior is compatible and expected for low alloy steel. For the buttering area, this variation could be attributed to the chromium depletion in the regions adjacent the grain boundary. In addition, the open circuit potential of alloy 82 is the most negative among all alloys. It suggests that the smallest driving force was required to initiate the corrosion of this alloy.

Table 5 – Corrosion parameters obtained from anodic polarization measurements.
The number in parenthesis are power of 10.

Sample	OCP(V)	i_{corr} (A/cm^2)	i_{crit} (A/cm^2)	i_{pass} (A/cm^2)	E_{pite} (V)
ASTM A-508	-0,471	2,85 (-4)	2,00 (-1)	2,05 (-4)	1,51
AISI 316L	-0,378	3,34 (-6)	3,67 (-5)	9,50 (-6)	0,902
Alloy 182	-0,237	2,51 (-6)	2,13 (-4)	2,00 (-6)	0,895
Alloy 82 buttering	-0,490	9,12 (-5)	1,00 (-3)	2,04 (-5)	0,885

icorr – corrosion current, icrit – critical current, ipass – passivation current, Epite – pite potential.

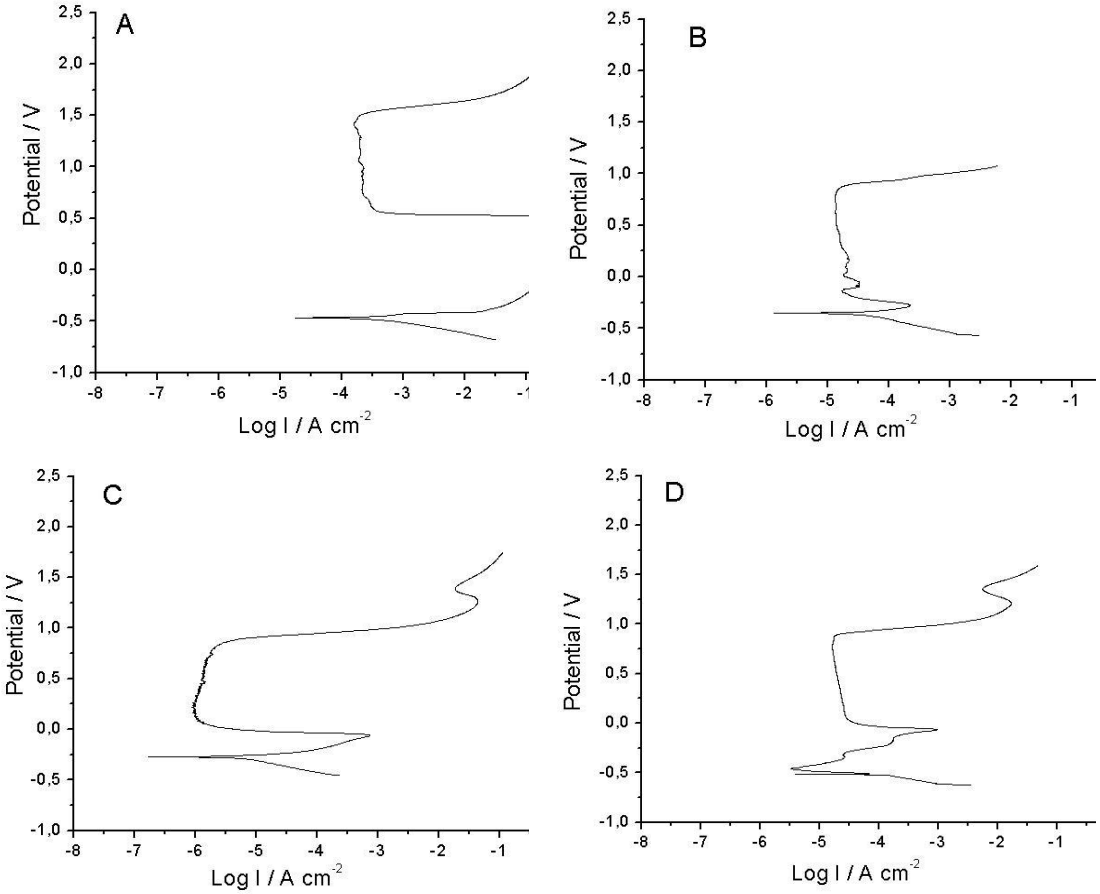

Figure 8 – Anodic polarization curves for the samples (A) ASTM A-508; (B) AISI 316, (C) Alloy 182; (D) Alloy 82 – Buttering area, in a de-aerated 0.5M H_2SO_4 solution.

5. CONCLUSIONS

The dissimilar welding procedure elaborated for joining dissimilar metals, allows to obtain a good compromise between microstructures and mechanical properties of different zones and regions of the welded joint showing good weldability, because the welds were well deposited and executed and presented a very well heaping up between each other.

The methodology utilized to elaborate the joining of dissimilar metals allowing to obtain a coherent microstructure with data available in the literature (Peng et al, 2007, Kaneda, 2007).

In the electrochemical tests conditions, the polarization curves indicated that alloy 82 has a weak passivity that could be attributed to the chromium depletion in the regions adjacent to the grain boundary. The results also indicated that the base metal ASTM A508 has the weakness passivity what is compatible and expected behavior for the low alloy steel.

6. ACKNOWLEDGEMENTS

The authors would acknowledge the Fundação de Amparo à Pesquisa do Estado de Minas Gerais – FAPEMIG, Financiadora de Estudos e Projetos – FINEP and the Eletronuclear- Eletrobrás Termonuclear S.A for the financial support provided for the work and Geraldo Antônio Scoralick Martins for the welding manufacturation.

7. REFERENCES

ASTM, G5 – 94 Standard reference test method for making potentiostatic and potentiodynamic polarization measurements, In: Annual book of ASTM standards, ASTM, West Conshohocken, United States.

ASTM E6 – 99 Standard guide for preparation of Metallographic specimens, In: Annual book of ASTM standards ASTM, West Conshohocken, United States.

ASTM E384 – 00 Standard Test Method for Microindentation Hardness of Materials, In: Annual book of ASTM standards ASTM, West Conshohocken, United States.

Bamford, W., Hall, J. A Review of Alloy 600 Cracking in Operating Nuclear Plants Including Alloy 82 and 182 Weld Behavior, Proc. 12th Int. Conf. on Nuclear Engineering, April 25-29, Arlington, Virginia USA, 2004.

EPRI - Electric Power Research Institute. Crack Growth Rates for Evaluating PWSCC of Alloy 82, 182 and 132 Welds. Material Reability Program - MRP 115, 2004. Accessed at: www.epriweb.com/public/000000000001006696.pdf.

Gomez-Briceño, D., Serrano, M. Aleaciones Base Niquel em Condiciones de Primario de Los Reactores Tipo PWR. Materiales, Março, 2005.

Kaneda, J., Horiuchi, T., Kuniya, J., Nagase, H., Koshiishi, M. Investigation of Precipitation and Segregation on Grain Boundaries in Ni-Based Alloys and Welds. Proc. 13th Int. Conf. on Nuclear Engineering, August 19-23, Whistler, British Columbia, 2007.

Le Canut, J.M, Maximovitch, S, Dalard, F. Electrochemical characterisation of nickel-based alloys in solutions at 320ºC. Journal of Nuclear Materials. 334, 2004, pp. 13-27.

Miteva, R., Taylor, N. G. General Review of Dissimilar Metal welding in Piping Systems of PWR Including WWER Designs. NESC – Network for evaluating Structural Components, NESCDOC (05) 007, 2005.

Pathania, R.S., Mcilree, A. R., Hickling, J. Overview of Primary Water Cracking of alloys 182/82 in PWRS. 5th Fontevraud Conference "Contribution of Material Investigation to the Resolution of Problems Encountered in Pressurized Water Reactors", CD-ROM, Fontevraud, Frankreich, 22-27. September 2002.

Peng, Q., Tetsuo, S., Yamauchi, H., Takeda, Y. Intergranular environmentally assisted cracking of Alloy 182 weld metal in simulated normal water chemistry of boiling water reactor. Corrosion science. 49, 2007, pp. 2767-2780.

Rebak, R.B. Environmentally Assisted Cracking of Commercial Ni-Cr-Mo alloys A review. Conference: Presented at: CORROSION/2005 and NACE Expo, Houston, TX (US), 04/03/2005--04/07/2005; Paper number 05457

Scott, P.M. An Overview of Materials Degradation by Stress Corrosion in PWRs. Eurocorr- Annual European Corrosion Conference of the European Federation of Corrosion, Nice, Acropolis, 12 – 16 of September, 2004.

Sireesha, M., Shankar, V., Albert, Shaju K., Sundaresan, S. Microstructural features of dissimilar welds between 316LN austenitic stainless steel and alloy 800. Materials Science and Engineering. A292, 2000, pp. 74-82

8. RESPONSIBILITY NOTICE

The authors are the only responsible for the printed material included in this paper.